Inorganic Chemistry
Article

Inorg. Chem. **2009**, *48*, 11809–11820 **11809**
DOI: 10.1021/ic901855x

Syntheses, Crystal Structures, and Properties of Five New Transition Metal Molybdenum(VI) Selenites and Tellurites

Su-Yun Zhang,[†,‡] Hai-Long Jiang,[†,‡] Chuan-Fu Sun,[†] and Jiang-Gao Mao*[,†]

[†]*State Key Laboratory of Structural Chemistry, Fujian Institute of Research on the Structure of Matter, Chinese Academy of Sciences, Fuzhou 350002, P.R. China, and* [‡]*Graduate School of the Chinese Academy of Sciences, Beijing, 100039, P.R. China*

Received September 19, 2009

Five new transition metal molybdenum(VI) selenites or tellurites, namely, $TM(MoO_3)(SeO_3)(H_2O)$ (TM = Mn, Co), $Fe_2(Mo_2O_7)(SeO_3)_2(H_2O)$, $Cu_2(MoO_4)(SeO_3)$, and $Ni_3(MoO_4)(TeO_3)_2$, have been prepared and structurally characterized. They belong to five different types of structures. $Mn(MoO_3)(SeO_3)(H_2O)$ and $Ni_3(MoO_4)(TeO_3)_2$ are non-centrosymmetric and crystallize in the orthorhombic space groups $Pmc2_1$ and $P2_12_12_1$, respectively, whereas $Co(MoO_3)(SeO_3)(H_2O)$, $Fe_2(Mo_2O_7)(SeO_3)_2(H_2O)$, and $Cu_2(MoO_4)(SeO_3)$ are centrosymmetric and crystallize in $P\bar{1}$, $C2/c$, $P2_1/c$, respectively. The Mo^{6+} cations in $Mn(MoO_3)(SeO_3)(H_2O)$, $Co(MoO_3)(SeO_3)(H_2O)$, and $Fe_2(Mo_2O_7)(SeO_3)_2(H_2O)$ are in severely distorted octahedral geometry whereas those in $Cu_2(MoO_4)(SeO_3)$ and $Ni_3(MoO_4)(TeO_3)_2$ are in a slightly distorted tetrahedral geometry. Second-Harmonic Generation (SHG) measurements revealed that $(MoO_3)(SeO_3)(H_2O)$ displays a moderate SHG signal of about $3 \times KH_2PO_4$ (KDP) whereas the SHG response of $Ni_3(MoO_4)(TeO_3)_2$ is much weaker than that of KDP.

Introduction

The search for new second-order nonlinear optical (NLO) materials is of current interest and great importance because of their applications in photonic and laser technologies.[1] The structural prerequisite for a second-order NLO material is that it is crystallographically non-centrosymmetric (NCS).[2] In inorganic materials, such compounds can be found in systems containing cations which are susceptible to second-order Jahn−Teller distortions, such as those with a stereo-active lone pair (Se^{4+},Te^{4+}, I^{5+}), or transition-metal ions with a d^0 electronic configuration (Ti^{4+}, V^{5+}, Nb^{5+}, W^{6+}, Mo^{6+}) in a distorted octahedral geometry.[3−6] It is reported that the combination of above two types of cations in the same compound can lead to compounds with enhanced Second-Harmonic Generation (SHG) properties because of the "constructive" addition of polarizations of both types of bonds.[7−10] So far, most of such studies were focused on A(Ae)-d^0 TM-Te^{IV} (or Se^{IV})-O systems which are usually insulators.[11−13] Recent studies in our group indicate that lanthanide(III) compounds containing both selenite (or tellurite) and molybdate (or tungstate) anions are normally not SHG active because of the higher coordination numbers for the lanthanide(III) ions; however, they are able to exhibit strong luminescence in the UV, visible, and near-IR regions.[14]

---

*To whom correspondence should be addressed. E-mail: mjg@fjirsm.ac.cn.

(1) Chen, C.; Liu, G. *Annu. Rev. Mater. Sci.* **1986**, *16*, 203.

(2) Nye, J. F. *Physical Properties of Crystals*; Oxford University Press: Oxford, 1957.

(3) Kong, F.; Huang, S. P.; Sun, Z. M.; Mao, J. G.; Cheng, W. D. *J. Am. Chem. Soc.* **2006**, *128*, 7750.

(4) (a) Goodey, J.; Broussard, J.; Halasyamani, P. S. *Chem. Mater.* **2002**, *14*, 3174. (b) Ok, K. M.; Halasyamani, P. S. *Chem. Mater.* **2001**, *13*, 4278.

(5) (a) Ok, K. M.; Orzechowski, J.; Halasyamani, P. S. *Inorg. Chem.* **2004**, *43*, 964. (b) Goodey, J.; Ok, K. M.; Broussard, J.; Hofmann, C.; Escobedo, F. V.; Halasyamani, P. S. *J. Solid State Chem.* **2003**, *175*, 3.

(6) (a) Harrison, W. T. A.; Dussack, L. L.; Jacobson, A. J. *J. Solid State Chem.* **1996**, *125*, 234. (b) Johnston, M. G.; Harrison, W. T. A. *Inorg. Chem.* **2001**, *40*, 6518. (c) Balraj, V.; Vidyasagar, K. *Inorg. Chem.* **1999**, *38*, 3458.

(7) (a) Porter, Y.; Bhuvanesh, N. S. P.; Halasyamani, P. S. *Inorg. Chem.* **2001**, *40*, 1172. (b) Porter, Y.; Ok, K. M.; Bhuvanesh, N. S. P.; Halasyamani, P. S. *Chem. Mater.* **2001**, *13*, 1910.

(8) (a) Sun, C. F.; Hu, C. L.; Xu, X.; Ling, J. B.; Hu, T.; Kong, F.; Long, X. F.; Mao, J. G. *J. Am. Chem. Soc.* **2009**, *131*, 9486. (b) Zhou, Y.; Hu, C. L.; Hu, T.; Kong, F.; Mao, J.-G. *Dalton Trans.* **2009**, 5747. (c) Mao, J.-G.; Jiang, H.-L.; Kong, F. *Inorg. Chem.* **2008**, *47*, 8498.

(9) (a) Ok, K. M.; Bhuvanesh, N. S. P.; Halasyamani, P. S. *Inorg. Chem.* **2001**, *40*, 1978. (b) Ok, K. M.; Bhuvanesh, N. S. P.; Halasyamani, P. S. *J. Solid State Chem.* **2001**, *161*, 57.

(10) (a) Chang, H. Y.; Kim, S. H.; Ok, K. M.; Halasyamani, P. S. *J. Am. Chem. Soc.* **2009**, *131*, 6865. (b) Chang, H. Y.; Kim, S. H.; Halasyamani, P. S.; Ok, K. M. *J. Am. Chem. Soc.* **2009**, *131*, 2426.

(11) (a) Ra, H. S.; Ok, K. M.; Halasyamani, P. S. *J. Am. Chem. Soc.* **2003**, *125*, 7764. (b) Ok, K. M.; Halasyamani, P. S. *Inorg. Chem.* **2004**, *43*, 4248.

(12) Hart, R. T.; Ok, K. M.; Halasyamani, P. S.; Zwanziger, J. W. *Appl. Phys. Lett.* **2004**, *85*, 938.

(13) Balraj, V.; Vidyasagar, K. *Inorg. Chem.* **1999**, *38*, 5809.

(14) (a) Shen, Y. L.; Jiang, H. L.; Xu, J.; Mao, J. G.; Cheah, K. W. *Inorg. Chem.* **2005**, *44*, 9314. (b) Jiang, H. L.; Ma, E.; Mao, J. G. *Inorg. Chem.* **2007**, *46*, 7012.

Reports on transition metal selenites or tellurites with additional d^0 transition metal ions are still rare.[8b,15,16] Several phases in $Zn^{II}/Cd^{II}-V^{V}-Se^{IV}/Te^{IV}-O$ system have been reported in our laboratory, among which $Cd_4V_2Te_3O_{15}$ displays a moderately SHG response of 1.4 times that of KH_2PO_4 (KDP).[15b,c] Furthermore, $Ni_3(Mo_2O_8)(SeO_3)$ and $Ni_3(Mo_2O_8)(TeO_3)$ with interesting ferromagnetic properties have also been reported.[15a]

We believe that more systematic investigations on the TM-d^0TM-Te^{IV}(or Se^{IV})-O systems may lead to more SHG and magnetic materials and provide further insights on their structure−property relationships. Our systematic explorations of new SHG materials in the TM-$Mo^{VI}-Se^{IV}/Te^{IV}-O$ system afforded five new transition metal molybdenum(VI) selenites or tellurites, namely, $TM(MoO_3)(SeO_3)(H_2O)$ (TM = Mn, Co), $Fe_2(Mo_2O_7)(SeO_3)_2(H_2O)$, $Cu_2(MoO_4)(SeO_3)$, and $Ni_3(MoO_4)(TeO_3)_2$. $Mn(MoO_3)(SeO_3)(H_2O)$ displays a moderately strong SHG efficiency of about 3 times that of KDP whereas the SHG signal of $Ni_3(MoO_4)(TeO_3)_2$ is much weaker than that of KDP. Herein we report their syntheses, crystal structure, optical properties, as well as magnetic properties.

Experimental Section

Materials and Methods. All of the chemicals were analytically pure, obtained from commercial sources, and used without further purification. Transition-metal oxides, manganous carbonate, cobalt(II) chloride were purchased from the Shanghai Reagent Factory, and SeO_2 (99+ %) and TeO_2 (99+ %) were purchased from ACROS ORGANICS. NiO was synthesized by heating Ni_2O_3 in air at 610 °C for 12 h, and its purity was checked by X-ray powder diffraction (XRD). Microprobe elemental analyses were performed on a field emission scanning electron microscope (FESEM, JSM6700F) equipped with an energy dispersive X-ray spectroscope (EDS, Oxford INCA). The XRD data were collected on a Panalytical X'pert Pro MPD diffractometer using graphite-monochromated Cu Kα radiation in the 2θ range of 5−65° with a step size of 0.02°. The absorption spectra were determined by the diffuse-reflection technique.[17a] $F(R)$ and R are linked by $F(R) = (1 - R)^2/2R$,[17b] where R is reflectance and $F(R)$ is the Kubelka−Munk remission function. The minima in the second derivative curves of the Kubelka−Munk function are taken as the position of the absorption bands. TGA studies were all carried out with NETZSCH STA 449C instruments. The sample and reference (Al_2O_3) were enclosed in a platinum crucible and heated at a rate of 10 °C/min from room temperature to 1000 °C under a nitrogen atmosphere. The IR spectra were recorded on a Magna 750 FT-IR spectrometer as KBr pellets in the range of 4000−400 cm^{-1}. $BaSO_4$ plate was used as a standard (100% reflectance). The measurements of the powder frequency-doubling effects were carried out by means of the method of Kurtz and Perry.[18] The fundamental wavelength is 1064 nm generated by a Q-switched Nd:YAG laser. The SHG wavelength is 532 nm. KDP was used as reference to assume the effect. Magnetic susceptibility measurements on polycrystalline samples were performed with a PPMS-9T magnetometer at a field of at 1000 or 5000 Oe in the temperature range 2−300 K. The raw data were corrected for the susceptibility of the container and the diamagnetic contributions of the samples using pascal's constants.[19]

Preparation of $Mn(MoO_3)(SeO_3)(H_2O)$. A mixture of 0.4 mmol MoO_3, 0.4 mmol $MnCO_3$, 1.2 mmol SeO_2, and H_2O (5 mL) was sealed in an autoclave equipped with a Teflon linear (23 mL) and heated at 210 °C for 4 days, followed by slow cooling to room temperature at a rate of 6 °C/h. Yellow brick-shaped crystals of $Mn(MoO_3)(SeO_3)(H_2O)$ were recovered. The energy-dispersive spectrometry (EDS) elemental analyses gave the molar ratio of Mn/Mo/Se of 1.0:1.3:1.3, which is in good agreement with the one determined from single crystal X-ray structural analysis. After proper structural analysis, $Mn(MoO_3)(SeO_3)(H_2O)$ was obtained as a single-phase by the reaction of a mixture of 0.4 mmol MoO_3, 0.4 mmol $MnCO_3$, and 0.4 mmol SeO_2 in 5 mL H_2O at 210 °C for 4 days. The yield is about 40% (based on Mo), and its purity was confirmed by XRD studies (Supporting Information). IR data (KBr, cm^{-1}): 3147(s), 1635 (s), 941 (w), 914 (s), 896 (s), 852 (m), 821 (m), 727 (m), 688(s), 584(s), 509(s).

Preparation of $Co(MoO_3)(SeO_3)(H_2O)$. A mixture of 0.4 mmol MoO_3, 0.4 mmol $CoCl_2$, 1.2 mmol SeO_2, and H_2O (5 mL) was sealed in an autoclave equipped with a Teflon linear (23 mL) and heated at 210 °C for 4 days, followed by slow cooling to room temperature at a rate of 6 °C/h. Brown plate-shaped crystals of $Co(MoO_3)(SeO_3)(H_2O)$ were recovered. The energy-dispersive spectrometry (EDS) elemental analyses gave the molar ratio of Co/Mo/Se of 1.0:1.3:1.4, which is in good agreement with the one determined from single crystal X-ray structural analysis. After proper structural analysis, $Co(MoO_3)(SeO_3)(H_2O)$ was obtained as a single-phase by the reaction of a mixture of 0.4 mmol MoO_3, 0.4 mmol $CoCl_2$, and 1.2 mmol SeO_2 in 5 mL of H_2O at 210 °C for 4 days. The yield is about 16% (based on Mo), and its purity was confirmed by XRD studies (Supporting Information). IR data (KBr, cm^{-1}): 3251(s), 3141 (s), 1571(m), 923 (s), 873 (s), 844 (s), 798 (w), 692 (m), 619 (s), 507 (s), 472(w).

Preparation of $Fe_2(Mo_2O_7)(SeO_3)_2(H_2O)$. A mixture of 0.4 mmol MoO_3, 0.4 mmol Fe_2O_3, 1.2 mmol SeO_2, and H_2O (5 mL) was sealed in an autoclave equipped with a Teflon linear (23 mL) and heated at 230 °C for 4 days, followed by slow cooling to room temperature at a rate of 6 °C/h. Red brick-shaped crystals of $Fe_2(Mo_2O_7)(SeO_3)_2(H_2O)$ were recovered. The energy-dispersive spectrometry (EDS) elemental analyses gave the molar ratio of Fe/Mo/Se of 1.0:1.3:1.1, which is in good agreement with the one determined from single crystal X-ray structural analysis. After proper structural analysis, $Fe_2(Mo_2O_7)(SeO_3)_2(H_2O)$ was obtained as a single-phase by the reaction of a mixture of 0.4 mmol MoO_3, 0.4 mmol Fe_2O_3, and 1.2 mmol SeO_2 in 5 mL of H_2O at 230 °C for 4 days. The yield is about 35% (based on Mo), and its purity was confirmed by XRD studies (Supporting Information). IR data (KBr, cm^{-1}): 3305(w), 1643(w), 1456(w), 962(s), 910 (s), 854 (s),744 (s), 663 (m), 601 (m), 507 (m), 460 (s).

Preparation of $Cu_2(MoO_4)(SeO_3)$. A mixture of 0.4 mmol MoO_3, 0.4 mmol CuO, 0.4 mmol SeO_2 and H_2O (5 mL) was sealed in an autoclave equipped with a Teflon linear (23 mL) and heated at 210 °C for 4 days, followed by slow cooling to room temperature at a rate of 6 °C/h. Green brick-shaped crystals of $Cu_2(MoO_4)(SeO_3)$ were recovered. The energy-dispersive spectrometry (EDS) elemental analyses gave the molar ratio of Cu/Mo/Se of 2.5:1.3:1.0, which is in good agreement with the one determined from single crystal X-ray structural analysis. After proper structural analysis, $Cu_2(MoO_4)(SeO_3)$ was obtained as a single-phase by the reaction of a mixture of 0.4 mmol MoO_3, 0.4 mmol CuO, 0.4 mmol SeO_2 in 5 mL H_2O at 210 °C for 4 days. The yield is about 31% (based on Mo), and its purity was confirmed by XRD studies (Supporting Information). IR data (KBr, cm^{-1}): 919(w), 869 (s), 806 (w), 711 (s),561 (m), 512 (m), 470 (m).

Preparation of $Ni_3(MoO_4)(TeO_3)_2$. Red prism-shaped crystals of $Ni_3(MoO_4)(TeO_3)_2$ were initially prepared by the high temperature solid-state reaction of a mixture of 0.64 mmol of NiO, 0.32 mmol of MoO_3, and 1.6 mmol of TeO_2. The reaction mixture was thoroughly ground and pressed into a pellet, which was then sealed into an evacuated quartz tube. The sample was allowed to

---

(15) (a) Jiang, H. L.; Xie, Z.; Mao, J. G. *Inorg. Chem.* **2007**, *46*, 6495. (b) Jiang, H. L.; Huang, S. P.; Fan, Y.; Mao, J. G.; Cheng, W. D. *Chem.—Eur. J.* **2008**, *14*, 1972. (c) Jiang, H. L.; Kong, F.; Fan, Y.; Mao, J. G. *Inorg. Chem.* **2008**, *47*, 7437.

(16) (a) Kim, Y. T.; Kim, Y. H.; Park, K.; Kwon, Y. U.; Young, V. G., Jr. *J. Solid State Chem.* **2001**, *161*, 23. (b) Halasyamani, P. S.; O'Hare, D. *Inorg. Chem.* **1997**, *36*, 6409.

(17) (a) Kubelka, P.; Munk, F. *Z. Tech. Phys.* **1931**, *12*, 593. (b) Wendlandt, W. W.; Hecht, H. G. *Reflectance Spectroscopy*; Interscience: New York, 1966.

(18) Kurtz, S. W.; Perry, T. T. *J. Appl. Phys.* **1968**, *39*, 3798.

(19) *Theory and Applications of Molecular Paramagnetism*; Boudreaux, E. A., Mulay, L. N., Eds.; John Wiley & Sons: New York, 1976.

Table 1. Crystal Data and Structure Refinements for the Title Compounds

formula	$H_2MnMoSeO_7$	$H_2CoMoSeO_7$	$H_2Fe_2Mo_2Se_2O_{17}$	Cu_2MoSeO_7	$Ni_3MoTe_2O_{10}$
fw	343.86	347.85	687.52	413.98	687.27
space group	$Pmc2_1$	$P\overline{1}$	$C2/c$	$P2_1/c$	$P2_12_12_1$
a/ Å	7.054(3)	4.974(4)	19.898(12)	8.148(5)	4.9475(2)
b/ Å	6.480(2)	6.614(5)	5.469(3)	9.023(5)	10.1781(5)
c/ Å	12.735(5)	8.876(6)	13.400(9)	8.392(5)	17.5579(10)
α/ deg	90	90.920(5)	90	90	90
β/ deg	90	98.092(9)	132.140(13)	104.675(12)	90
γ/ deg	90	110.385(12)	90	90	90
V/ Å^3	582.1(4)	270.3(4)	1081.3(12)	596.9(6)	884.15(8)
Z	4	2	4	4	4
D_{calcd}/g cm^{-3}	3.923	4.274	4.223	4.607	5.163
μ(Mo Kα)/mm^{-1}	10.553	12.096	11.710	15.213	14.185
GOF on F^2	1.025	1.041	1.024	1.112	1.058
R1, wR2 [$I > 2\sigma(I)$][a]	0.0239, 0.0462	0.0386, 0.0962	0.0240, 0.0538	0.0279, 0.0610	0.0169, 0.0383
R1, wR2 (all data)	0.0263, 0.0467	0.0416, 0.0991	0.0285, 0.0560	0.0309, 0.0619	0.0180, 0.0388

[a] $R1 = \sum||F_o| - |F_c||/\sum|F_o|$, $wR2 = \{\sum w(F_o^2 - F_c^2)^2/\sum w(F_o^2)^2\}^{1/2}$.

heat at 720 °C for 6 days, cooled to 270 at 4.5 °C/h before switching off the furnace. The energy-dispersive spectrometry (EDS) elemental analysis gave the molar ratio of Ni/Mo/Te of 3.2:1.0:2.2, which matches well with the one from single crystal X-ray structural analysis. After proper structural analysis, a pure sample of $Ni_3(MoO_4)(TeO_3)_2$ was obtained quantitatively by the reaction of a mixture of $NiO/MoO_3/TeO_2$ in a molar ratio of 3:1:2 at 720 °C for 6 days. Its purity was confirmed by XRD studies (See Supporting Information). IR data (KBr, cm^{-1}): 925(m), 863 (m), 779 (s), 692 (vs), 644 (vs), 517 (w), 472 (w), 435 (w).

X-ray Crystallography. Data collections for the above five compounds were performed on either a Rigaku Mercury CCD diffractometer (for $Co(MoO_3)(SeO_3)(H_2O)$, $Fe_2(Mo_2O_7)(SeO_3)_2(H_2O)$, $Cu_2(MoO_4)(SeO_3)$, and $Ni_3(MoO_4)(TeO_3)_2$) or SATURN 70 CCD diffractometer (for $Mn(MoO_3)(SeO_3)(H_2O)$) equipped with a graphite-monochromated Mo-Kα radiation ($\lambda = 0.71073$ Å) at 293 K. The data sets were corrected for Lorentz and polarization factors, as well as for absorption by Multiscan method.[20a] All five structures were solved by direct methods and refined by full-matrix least-squares fitting on F^2 by SHELX-97.[20b] All non-hydrogen atoms were refined with anisotropic thermal parameters. The hydrogen atoms associated with the aqua ligands were located at calculated positions and refined with isotropic thermal parameters. The O(10) atom in $Mn(MoO_3)(SeO_3)(H_2O)$ with relatively large thermal parameters was refined with a 50% occupancy factor. The refined Flack factors of 0.018(20) and 0.03(2) respectively for $Mn(MoO_3)(SeO_3)(H_2O)$ and $Ni_3(MoO_4)(TeO_3)_2$ confirmed the correctness of their absolute structures. Crystallographic data and structural refinements for the five compounds are summarized in Table 1. Important bond distances are listed in Table 2. More details on the crystallographic studies as well as atomic displacement parameters are given as Supporting Information.

Result and Discussion

Structural Descriptions. Explorations of the new types of second order NLO materials in the TM-Mo(VI)−Se(IV)/Te(IV)-O systems led to five new transition metal molybdenum(VI) selenites and tellurites, namely, $TM(MoO_3)(SeO_3)(H_2O)$ (TM = Mn, Co), $Fe_2(Mo_2O_7)(SeO_3)_2(H_2O)$, $Cu_2(MoO_4)(SeO_3)$, and $Ni_3(MoO_4)(TeO_3)_2$. They belong to five different types of structures.

Structure of $Mn(MoO_3)(SeO_3)(H_2O)$. The structure of $Mn(MoO_3)(SeO_3)(H_2O)$ features a complicated three-dimensional (3D) network composed of MnO_7 ployhedra, MoO_6 octahedra and SeO_3 polyhedra (Figure 1a). Its asymmetric unit contains two unique Mn atoms lying on mirror planes, one Mo in the general site and two Se atoms sitting on mirror planes. Both Mn(1) and Mn(2) are seven-coordinated by three selenite oxygens, one aqua ligand and four oxo anions with Mn−O distances ranging from 2.123(4) to 2.342(4) Å (Table 2). The coordination environment around the Mn^{2+} ions can be described as a pentagonal bipyramid. It should be noted that Mn^{2+} ions in most of the manganese(II) selenites or tellerites are octahedrally coordinated.[21] The Mo(VI) cation is octahedrally coordinated by two selenite oxygens, two terminal, and two bridging oxo anions. The Mo−O bond distances are in the range of 1.711(4)−2.210(3) Å (Table 2). Two Mo−O (oxygen atoms from SeO_3^{2-} groups) bonds are significantly longer than the remaining Mo−O bonds. The *trans* O−Mo−O angles are in the range of 154.0(2)−170.4(2)°, and those of the *cis* ones are in the range of 77.4(2)−101.7(2)°, both are significantly deviated from ideal 180 and 90°. Hence, the MoO_6 octahedra are severely distorted. Mo(1) is distorted toward O(5)···O(6) edge (local C_2 direction) with two "short" (1.711(4) and 1.715(4) Å), two "normal" (1.937(2) and 1.937(3) Å), and two "long" (2.177(4) and 2.210(3) Å) Mo−O bonds (Table 2). Taking into account the six Mo−O bond lengths as well as the deviations of the three *trans* O−Mo−O bond angles from 180°, the magnitudes of the distortion (Δd) was calculated to be 0.98 Å.[22] The distortion is away from the lone pair cation Se(IV), as in other metal selenites with distorted MoO_6 octahedra.[23] Both Se(IV) atoms are in a ψ-SeO_3 trigonal-pyramidal geometry with the lone pair of Se (IV) occupying the pyramidal site. The Se−O distances range from 1.679(6) to 1.731(4) Å (Table 2). Bond valence calculations indicate that Mn, Mo, and Se atoms are in oxidation states of +2, +6, and +4, respectively. The calculated total bond valences for the Mn(1), Mn(2), Mo(1), Se(1), and Se(2) atoms are 2.070, 2.059, 6.096, 3.976, and 3.931, respectively.[24]

---

(20) (a) *CrystalClear*, Version 1.3.5; Rigaku Corp.: Woodlands, TX, 1999. (b) Sheldrick, G. M. *SHELXTL, Crystallographic Software Package, SHELXTL, Version 5.1*; Bruker-AXS: Madison, WI, 1998.

(21) (a) Larranaga, A.; Mesa, J. L.; Pizarro, J. L.; Pena, A.; Olazcuaga, R.; Arriortua, M. I.; Rojo, T. *J. Solid State Chem.* **2005**, *178*, 3686. (b) Kohn, K.; Inoue, K.; Horie, O.; Akimoto, S. *J. Solid State Chem.* **1976**, *18*, 27. (c) Giester, G.; Wildner, M. *J. Solid State Chem.* **1991**, *91*, 370. (d) Shen, Y. L.; Mao, J. G. *Inorg. Chem.* **2005**, *44*, 5328. (e) Johnston, M. G.; Harrison, W. T. A. *Acta Crystallogr., Sect. E* **2002**, *58*, i59.

(22) (a) Halasyamani, P. -S. *Chem. Mater.* **2004**, *16*, 3586. (b) Porter, Y.; Halasyamani, P. S. *J. Solid State Chem.* **2003**, *174*, 441.

(23) (a) Balraj, V.; Vidyasagar, K. *Inorg. Chem.* **1998**, *37*, 4764. (b) Balraj, V.; Vidyasagar, K. *Inorg. Chem.* **1999**, *38*, 1394.

(24) (a) Guesdon, A.; Raveau, B. *Chem. Mater.* **2000**, *12*, 2239. (b) Chi, E. O.; Ok, K. M.; Porter, Y.; Halasyamani, P. S. *Chem. Mater.* **2006**, *18*, 2070.

The MoO_6 octahedra are interconnected via corner-sharing (O(8) and O(7)) into a one-dimensional (1D) Mo−O chain along the *a*-axis (Figure 1b). The interconnection of MnO_7 polyhedra by bridging SeO_3 groups resulted in a manganese(II) selenite chain along the *a*-axis. The shortest Mn···Mn separation is 5.137(1) Å. The above two types of chains are further interconnected and alternating along *b* and *c*-axes, forming a complicated 3D network with 1D tunnels of Mn_2Mo_2Se 5-member rings (MRs) and small tunnels of $MnMo_2$ 3-MR long the *b*-axis. The lone pair of Se(2) atom is located at 3-MR tunnels whereas that of Se(1) atom is orientated toward the centers of 5-MR tunnels. Both $Se(1)O_3$ and $Se(2)O_3$ are pentadentate, and each connects with three Mn and two Mo atoms, two oxygen atoms are bidentate, and each bridges with a Mn and Mo atoms whereas the third oxygen only bonds to a Mn atoms.

Table 2. Important Bond Lengths (Å) for the Five Compounds[a]

$Mn(MoO_3)(SeO_3)(H_2O)$			
Mn(1)−O(1)	2.119(6)	Mn(1)−O(10)#1	2.203(8)
Mn(1)−O(10)	2.203(8)	Mn(1)−O(5)#2	2.223(4)
Mn(1)−O(5)#3	2.223(4)	Mn(1)−O(7)	2.284(5)
Mn(1)−O(4)	2.345(3)	Mn(1)−O(4)#1	2.345(3)
Mn(2)−O(3)#4	2.117(5)	Mn(2)−O(9)	2.185(6)
Mn(2)−O(6)#5	2.253(4)	Mn(2)−O(6)	2.253(4)
Mn(2)−O(8)#4	2.269(5)	Mn(2)−O(2)#6	2.337(3)
Mn(2)−O(2)#4	2.337(3)	Mo(1)−O(6)	1.716(4)
Mo(1)−O(5)	1.717(4)	Mo(1)−O(7)	1.937(2)
Mo(1)−O(8)	1.940(2)	Mo(1)−O(2)	2.181(4)
Mo(1)−O(4)	2.211(3)	Se(1)−O(1)	1.677(5)
Se(1)−O(2)#1	1.721(3)	Se(1)−O(2)	1.721(3)
Se(2)−O(3)	1.683(6)	Se(2)−O(4)#5	1.726(3)
Se(2)−O(4)	1.726(3)		
$Co(MoO_3)(SeO_3)(H_2O)$			
Co(1)−O(1)#1	1.991(6)	Co(1)−O(1)	1.991(6)
Co(1)−O(6)#2	2.109(5)	Co(1)−O(6)#3	2.109(5)
Co(1)−O(2)#1	2.192(5)	Co(1)−O(2)	2.192(5)
Co(2)−O(5)#4	2.057(5)	Co(2)−O(5)	2.057(5)
Co(2)−O(4)#5	2.150(5)	Co(2)−O(4)#6	2.150(5)
Co(2)−O(3)	2.150(5)	Co(2)−O(3)#4	2.150(5)
Mo(1)−O(2)	1.712(5)	Mo(1)−O(3)	1.731(5)
Mo(1)−O(4)	1.871(5)	Mo(1)−O(7)#7	2.037(5)
Mo(1)−O(4)#2	2.138(5)	Mo(1)−O(7)	2.300(5)
Se(1)−O(6)	1.666(5)	Se(1)−O(5)	1.677(5)
Se(1)−O(7)	1.792(5)		
$Fe_2(Mo_2O_7)(SeO_3)_2(H_2O)$			
Fe(1)−O(8)#1	1.914(3)	Fe(1)−O(7)#2	1.981(3)
Fe(1)−O(5)#3	1.992(3)	Fe(1)−O(6)	2.020(3)
Fe(1)−O(4)#4	2.053(3)	Fe(1)−O(5)	2.073(3)
Mo(1)−O(2)	1.686(3)	Mo(1)−O(4)	1.732(3)
Mo(1)−O(5)	1.874(3)	Mo(1)−O(3)	1.9176(19)
Mo(1)−O(6)	2.319(3)	Mo(1)−O(1)	2.444(3)
Se(1)−O(8)	1.679(3)	Se(1)−O(7)	1.699(3)
Se(1)−O(6)	1.740(3)	Fe(1)−Fe(1)#5	3.142(2)
$Cu_2(MoO_4)(SeO_3)$			
Cu(1)−O(3)#1	1.930(4)	Cu(1)−O(4)	1.951(4)
Cu(1)−O(5)#2	1.980(4)	Cu(1)−O(1)	2.014(3)
Cu(1)−O(3)#3	2.252(4)	Cu(1)−Cu(2)	2.9727(19)
Cu(2)−O(2)#4	1.928(3)	Cu(2)−O(4)	1.958(3)
Cu(2)−O(7)#5	1.959(4)	Cu(2)−O(1)	1.995(4)
Cu(2)−O(2)#3	2.252(4)	Mo(1)−O(6)	1.730(4)
Mo(1)−O(5)	1.745(3)	Mo(1)−O(7)	1.748(4)
Mo(1)−O(4)	1.837(3)	Se(1)−O(3)	1.690(3)
Se(1)−O(2)	1.695(3)	Se(1)−O(1)	1.728(3)
Cu(1)−Cu(2)#6	2.973(2)		
Cu(1)−Cu(1)#7	3.186(2)	Cu(2)−Cu(2)#8	3.149(5)
$Ni_3(MoO_4)(TeO_3)_2$			
Ni(1)−O(4)	1.990(3)	Ni(1)−O(5)#1	2.034(3)
Ni(1)−O(1)#2	2.044(3)	Ni(1)−O(7)	2.063(3)
Ni(1)−O(2)#2	2.084(3)	Ni(1)−O(3)#3	2.115(3)
Ni(2)−O(3)	2.022(3)	Ni(2)−O(9)	2.033(3)
Ni(2)−O(2)	2.043(3)	Ni(2)−O(5)#4	2.068(3)
Ni(2)−O(1)#5	2.072(3)	Ni(2)−O(7)#6	2.075(3)
Ni(3)−O(4)	1.974(3)	Ni(3)−O(8)#7	2.031(4)
Ni(3)−O(9)#2	2.035(3)	Ni(3)−O(6)#8	2.044(3)
Ni(3)−O(6)#1	2.055(3)		
Mo(1)−O(10)	1.674(4)	Mo(1)−O(8)#3	1.761(3)
Mo(1)−O(9)#3	1.806(3)	Mo(1)−O(7)	1.817(3)
Te(1)−O(1)	1.874(3)	Te(1)−O(3)	1.876(3)
Te(1)−O(2)#1	1.892(3)	Te(2)−O(4)	1.877(3)
Te(2)−O(6)	1.887(3)	Te(2)−O(5)	1.887(3)
Ni(1)−Ni(2)#3	3.037(0)	Ni(1)−Ni(2)#10	3.064(0)
Ni(1)−Ni(2)#2	3.592(0)	Ni(1)−Ni(3)	3.170(0)
Ni(2)−Ni(3)#5	3.395(0)	Ni(3)−Ni(3)#8	3.464(0)
Ni(3)−Ni(3)#9	3.464(0)		

[a] Symmetry transformations used to generate equivalent atoms: For $Mn(MoO_3)$ (SeO_3) (H_2O): #1 $-x,y,z$, #2 $-x,y-1,z$, #3 $x,y-1,z$, #4 $-x+1,-y+2,z-1/2$, #5 $-x+1,y,z$, #6 $x,-y+2,z-1/2$, #7 $-x+1,-y+2,z+1/2$, #8 $x,y+1,z$; For $Co(MoO_3)$ (SeO_3) (H_2O): #1 $-x+1,-y+1,-z+1$, #2 $-x,-y+1,-z+1$, #3 $-x+1,-y,-z+1$, #4 $-x,-y,-z+1$, #5 $x+1,y,z$, #6 $-x,-y+1,-z+2$, #7 $x,y,z+1$, #8 $x-1,y,z$, #9 $x, y, z-1$; For $Fe_2(Mo_2O_7)(SeO_3)_2(H_2O)$: #1 $-x+1/2, y-1/2, -z+1/2$, #2 $x, y-1, z$, #3 $-x+1/2, -y-1/2, -z+1$, #4 $-x+1/2,-y+1/2,-z+1$, #5 $-x+1/2,-y-1/2,-z+1$; For $Cu_2(MoO_4)(SeO_3)$: #1 $x, -y-1/2, z+1/2$, #2 $x, -y+1/2, z+1/2$, #3 $-x+1, y+1/2, -z+1/2$, #4 $x,-y-1/2, z-1/2$, #5 $x, -y+1/2, z-1/2$, #6 $-x+1,y-1/2,-z+1/2$, #7 x, y, z, #8 $-x+1, -y, -z+1$; For $Ni_3(MoO_4)(TeO_3)_2$: #1 $x+1, y, z$; #2 $-x+1, y+1/2, -z+1/2$; #3 $x, y+1, z$; #4 $x, y-1, z$; #5 $-x+1, y-1/2, -z+1/2$; #6 $x-1, y-1, z$; #7 $-x+2, y+1/2, -z+1/2$; #8 $x+1/2, -y+3/2, -z+1$; #9 $x-1/2, -y+3/2, -z+1$; #10 $x+1, y+1, z$.

Structure of $Co(MoO_3)(SeO_3)(H_2O)$. The structure of $Co(MoO_3)(SeO_3)(H_2O)$ features a 3D network with 1D 8-MR tunnels along the *a* axis (Figure 2a). The asymmetric unit of $Co(MoO_3)(SeO_3)(H_2O)$ is composed of two Co atoms on inversion centers, one Mo, one SeO_3^{2-} anion, and an aqua ligand on general sites. Both Co(1) and Co(2) are octahedrally coordinated by six oxygen atoms. The coordination geometry around Co(1) composes of two selenite anions in a unidentate fashion, two oxo anions, and two aqua ligands whereas Co(2) is surrounded by two selenite anions in a unidentate fashion and four oxo anions. The Co−O distances are in the range of 2.001(6) to 2.191(5) Å (Table 2). The Mo(1) atom is octahedrally coordinated by two selenite oxygens, two terminal and two bridging oxo anions. Different from $Mn(MoO_3)(SeO_3)(H_2O)$, the MoO_6 octahedron in $Co(MoO_3)(SeO_3)(H_2O)$ exhibits three "short" Mo−O (1.712(5)−1.866(5) Å) and three "long" Mo−O (2.038(5)−2.300(5) Å) bonds. Hence, the Mo(VI) cation is distorted toward a face formed by O(2), O(3), and O(4) atoms (local C_3 direction), the distortion is away from the lone pair containing Se(IV) cations as reported in other metal selenites with distorted MoO_6 octahedra.[23] The *trans* O−Mo−O angles are in the range of 150.5(2)−166.3(2)° whereas those of the *cis* ones in the range of 76.3(2)−106.4(2)°. The magnitude of the distortion (Δd) was calculated to be 1.248 Å.[22] The Se(IV) cations are coordinated by three oxygen atoms in a distorted ψ-SeO_3 trigonal-pyramidal geometry with the lone pair of Se(IV) occupying the pyramidal site. The Se−O distances fall in the normal range of 1.666(5)−1.791(5) Å (Table 2). Bond valence calculations indicate that Co, Mo, and Se atoms

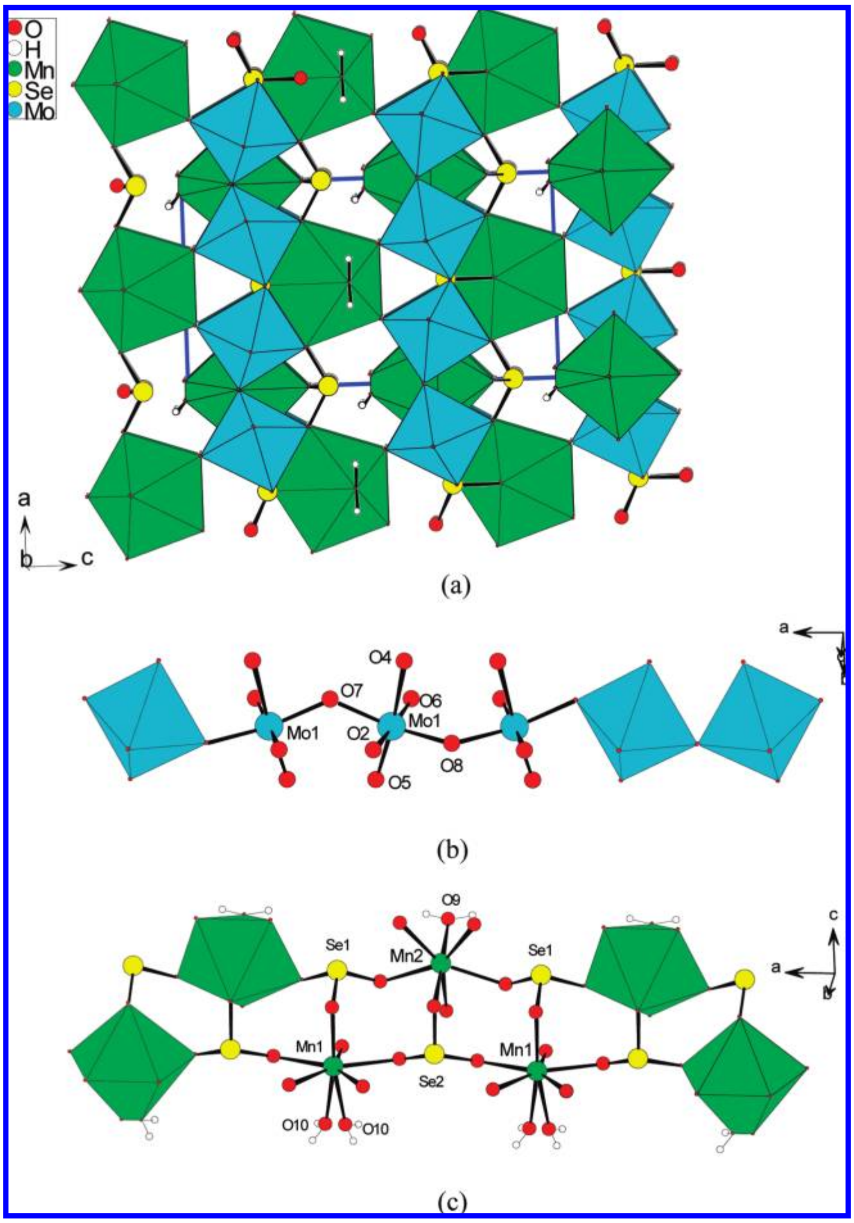

Figure 1. View the structure of $Mn(MoO_3)(SeO_3)(H_2O)$ down the *b*-axis (a); a 1D molybdenum(VI) oxide chain (b), and a manganese(II) selenite chain (c) along *a*-axis.

are in oxidation states of +2, +6, and +4, respectively. The calculated total bond valences for Co(1), Co(2), Mo(1), and Se(1) atoms are 2.059, 1.901, 6.018, and 3.937, respectively.[24]

The MoO_6 octahedra are interconnected into a 1D chain along the *a*-axis through edge-sharing (O(4)···O(4) and O(7)···O(7)), the selenite anions are hanging on both sides of the chain (Figure 2b). Co(2)O_6 and Co(1)O_6 octahedra are bridged by selenite groups into a 1D chain along ⟨011⟩ direction (Figure 2c). The Co···Co separation of the Co−O−Se−O−Co bridge is 6.317(1) Å. The above two types of chains are further interconnected via Co−O−Mo, Co−O−Se, and Mo−O−Se bridges into a 3D network with 1D 8-MR tunnels along the *a* axis. The Se(1)O_3 group serves as a tetradentate metal linker and bonds to two Co and two Mo atoms; O(7) is bidentate whereas O(5) and O(6) are monodentate. The lone pair electrons of the Se(IV) cations are orientated toward the center of the tunnels. Alternatively, the structure of $Co(MoO_3)(SeO_3)(H_2O)$ can be described as a 3D network built by corner and edge sharing CoO_6 and MoO_6 octahedra with 1D 8-MR tunnels capped by Se(IV) atoms.

It is interesting to note that though $Mn(MoO_3)(SeO_3)(H_2O)$ and $Co(MoO_3)(SeO_3)(H_2O)$ have the similar formulae they exhibit two different types of 3D structures. The main differences are in three aspects. First, the coordination geometries around Mn^{2+} and Co^{2+} are different: Mn^{2+} is seven-coordinated with a pentagonal bipyramidal geometry whereas Co^{2+} is octahedrally coordinated. Second, the 1D molybdenum(VI) oxide chain in $Co(MoO_3)(SeO_3)(H_2O)$ is based on edge-sharing MoO_6 octahedra whereas the one in $Mn(MoO_3)(SeO_3)(H_2O)$ is composed of corner-sharing MoO_6 octahedra. Furthermore, the coordination modes of the selenite anions in both compounds are different: the selenite

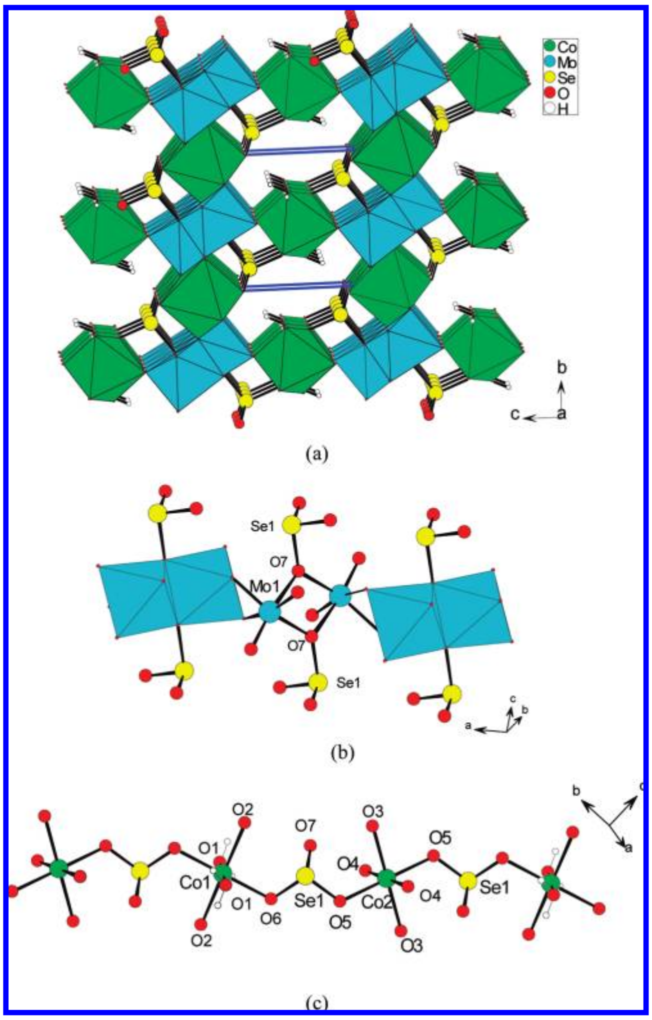

Figure 2. View of the structure of $Co(MoO_3)(SeO_3)(H_2O)$ down the *a*-axis (a), a 1D molybdenum(VI) selenite chain along the *a* axis (b), and a 1D cobalt(II) selenite chain along the (0 1 −1) direction (c).

anions in the Mn compound are pentadentate whereas those in the Co compound are tetradentate.

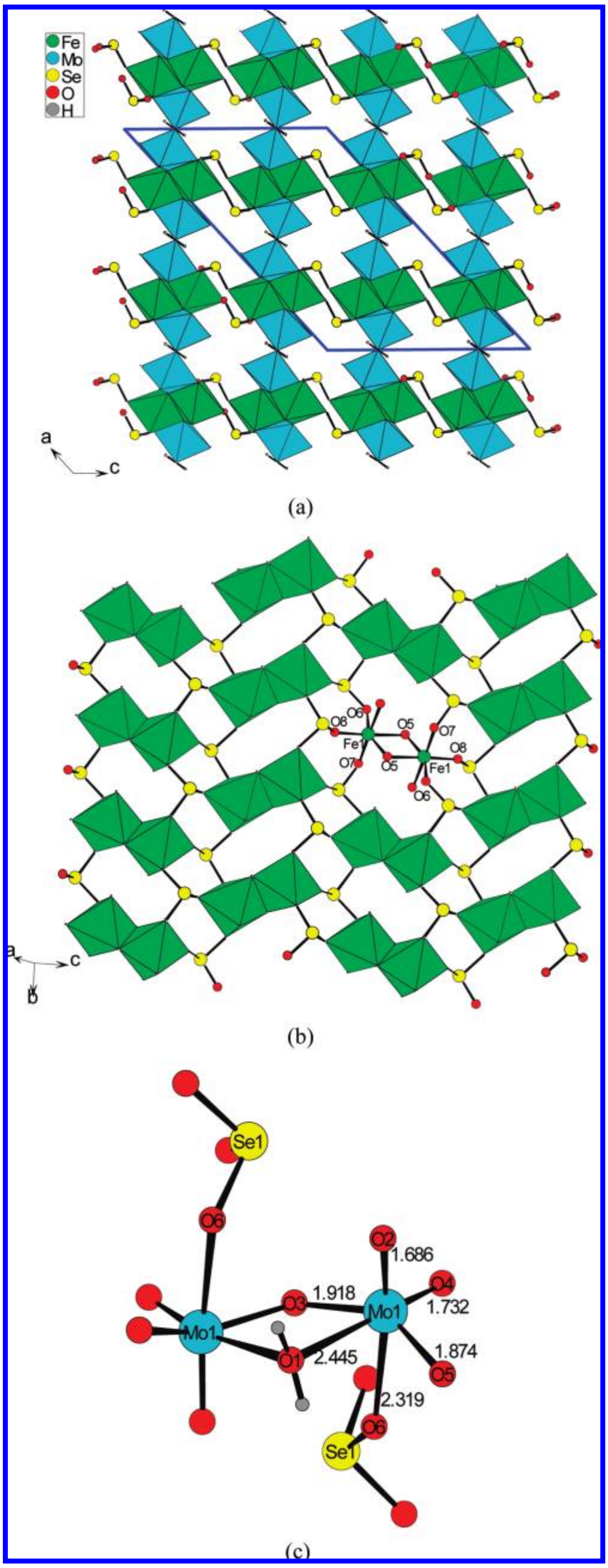

Figure 3. View of the structure of $Fe_2(Mo_2O_7)(SeO_3)_2(H_2O)$ down the *b*-axis (a), a 2D iron(III) selenite layer parallel to the *bc* plane (b), and a $Mo_2O_9(H_2O)$ dimeric unit (c) in $Fe_2(Mo_2O_7)(SeO_3)_2(H_2O)$.

Structure of $Fe_2(Mo_2O_7)(SeO_3)_2(H_2O)$. The structure of $Fe_2(Mo_2O_7)(SeO_3)_2(H_2O)$ is isostructural to $In_2(Mo_2O_7)(SeO_3)_2(H_2O)$ and features a pillared-layered architecture composed of iron(III) selenite layers interconnected by Mo_2O_{10} dimers (Figure 3a).[25] The asymmetric unit of $Fe_2(Mo_2O_7)(SeO_3)_2(H_2O)$ contains one Fe, one Mo, and one selenite group. The Fe^{3+} ion is octahedrally coordinated by six oxygen atoms with the Fe−O distances ranging from 2.072(3) to 1.916(3) Å (Table 2). The Mo(VI) cation is octahedrally coordinated by one selenite oxygen, one terminal oxygen, an aqua ligand, and three oxo anions. The Mo−O bond distances are in the range of 1.683(3)−2.450(3) Å (Table 2). The *trans* O−Mo−O angles fall the range of 143.0(1)−168.2(1)° whereas the *cis* O−Mo−O angles in the range of 71.2(1)−104.4(1)°. The MoO_6 octahedron is distorted toward the O(5)···O(7) edge (local C_2 direction), displaying two "short" (1.683(3), 1.730(3)Å), two "normal" (1.875(3), 1.9169(19) Å), and two "long" (2.319(3), 2.450(3) Å) Mo−O bonds (Table 2). The magnitudes of the distortion (Δd) was calculated to be 1.45 Å,[22] which is comparable to that in $In_2(Mo_2O_7)(SeO_3)_2(H_2O)$. The distortion is also

---

[25] Kong, F.; Lin, Q. P.; Yi, F. Y.; Mao, J. G. *Inorg. Chem.* **2009**, *48*, 6794.

away from the lone pair cation Se(IV) as expected.[23] The Se (IV) atom is in a ψ-SeO_3 trigonal-pyramidal geometry with the lone pair of Se (IV) occupying the pyramidal site. The Se−O distances range from 1.679(3) to 1.741(3) Å (Table 2). Bond valence calculations indicate that Fe, Mo, and Se atoms are in oxidation states of +3, +6, and +4, respectively. The calculated total bond valences for Fe(1), Mo(1), and Se(1) atoms are 2.910, 6.049, and 3.994, respectively.[24]

Each pair of FeO_6 octahedra form Fe_2O_{10} dimers via edge-sharing (O(5)···O(5)), the dimers are further bridged by selenite anions into a ⟨1 0 0⟩ layer (Figure 3b). The Fe···Fe separation within a Fe_2O_{10} dimer is 3.142(1) Å, and the one of the Fe−O−Se−O−Fe bridge is 4.715(1) Å. Two MoO_6 octahedra form a Mo_2O_{10} dimer by edge-sharing (O(1)···O(3)) (Figure 3c). It is noted that O(3) is an O^{2-} anion whereas O(1) is an aqua ligand. The above iron(III) selenite layers are further interconnected by the Mo_2O_{10} dimers via Mo−O−Fe bridges into a 3D framework with 1D 8-MR tunnels along the *b*-axis. The 8-MR is composed of 2 SeO_3, 2 FeO_6, and 4 MoO_6 groups. The lone pairs of the selenite groups are orientated toward the centers of the above tunnels. The Se(1)O_3 group serves as a tetradentate metal linker, bridging with three Fe(1) and one Mo(1) atoms.

Structure of $Cu_2(MoO_4)(SeO_3)$. $Cu_2(MoO_4)(SeO_3)$ exhibits a two-dimensional (2D) layer structure in which the 1D copper(II) oxide chains are further bridged by SeO_3^{2-} and MoO_4^{2-} groups (Figure 4). Its asymmetric unit contains two Cu, one Mo, and one Se atoms. Both Cu(1) and Cu(2) are 5-coordinated by three selenite oxygens and two O^{2-} anions in a square pyramidal geometry. The Cu−O distances range from 1.930(4) to 2.252(4) Å (Table 2). The Mo(VI) cation is in a tetrahedral geometry composed of four oxo anions with Mo−O distances ranging from 1.730(4) to 1.837(3) Å (Table 2). The Se(IV) atom is coordinated by three oxygen atoms in a distorted ψ-SeO_3 tetrahedral geometry, with the fourth site occupied by the lone-pair electrons with Se−O distances ranging from 1.690(3) to 1.728(3) Å (Table 2). Bond valence calculations indicate that Cu, Mo, and Se atoms are in oxidation states of +2, +6, and +4, respectively. The calculated total bond valences for the Cu(1), Cu(2), Mo(1), and Se(1) atoms are 2.047, 2.090, 5.908, and 4.010, respectively.[24]

Cu(1)O_5 and Cu(2)O_5 square pyramids are interconnected via edge-sharing (O(3)···O(3), O(2)···O(2), and O(1)···O(4)) into a copper(II) oxide chain along the *c*-axis (Figure 4c). The Cu(1)···Cu(2) separation of 2.9729(17) Å is significantly shorter than the Cu(1)···Cu(1) (3.186(2) Å) and Cu(2)···Cu(2) (3.149(2) Å) distances. The Cu−O−Cu angles are in the range of 95.62(1)−99.00(1)°.

Neighboring copper oxide chains are bridged by SeO_3 and MoO_4 groups via corner-sharing into a 2D layer parallel to the *bc* plane with 1D 5-MR tunnels along the *c*-axis (Figure 4a). The lone-pair electrons of the Se(IV) atoms are orientated toward the interlayer space. The interlayer *d*-spacing is about 8.15 Å. The selenite anion is hexadentate and bridges with six Cu atoms, all three oxygen atoms are bidentate.

Structure of $Ni_3(MoO_4)(TeO_3)_2$. $Ni_3(MoO_4)(TeO_3)_2$ was synthesized by solid state reactions at 720 °C: $3NiO + MoO_3 + 2TeO_2 \rightarrow Ni_3(MoO_4)(TeO_3)_2$. It features a 3D network in which the TeO_3^{2-} and MoO_4^{2-} anions are capped on the walls of the 1D tunnels of nickel(II) oxide (Figure 5a). The asymmetric unit of $Ni_3(MoO_4)(TeO_3)_2$ contains three independent Ni, one Mo, and two Te atoms in general sites. Ni(1) is octahedrally coordinated by six oxygens from one MoO_4^{2-} and five TeO_3^{2-} anions, Ni(2) is octahedrally coordinated by six oxygen atoms from two oxo anions and four TeO_3^{2-} anions, whereas Ni(3) is five-coordinated by five oxygen atoms from two oxo anions and three TeO_3^{2-} anions. The Ni−O distances are in the range of 1.974(3)−2.115(3) Å (Table 2). The Mo(VI) atom is in a tetrahedral coordination environment with Mo−O distances ranging from 1.674(4) to 1.817(3) Å (Table 2). Both Te(1) and Te(2) atoms are in a ψ-TeO_3 trigonal pyramidal geometry with the lone pair of Te (IV) occupying the pyramidal site. The Te−O distances range from 1.874(3) to 1.892(3) Å (Table 2). Bond valence calculations indicate that Ni, Mo, and Te atoms are in oxidation sates of +2, +6, and +4, respectively. The calculated total bond valences for Ni(1), Ni(2), Ni(3), Mo(1), Te(1), and Te(2) atoms are 2.04, 2.05, 1.83, 5.95, 3.89, and 3.86, respectively.[24]

Each Ni(1)O_6 octahedron connects with two neighboring Ni(2)O_6 octahedra via edge-sharing (O(1)···O(3) and O(5)···O(7)) to form a 1D chain along the *a*-axis. Neighboring such chains are interconnected via Ni(1)−O−Ni(2) bridges into a 2D nickel(II) oxide layer parallel to the *ab* plane (Figure 5b). Neighboring Ni(3)O_5 polyhedra are interconnected via corner-sharing (O(6)) into a right-hand helical chain along the *a*-axis (Figure 5c). The Ni(1,2)−O layers and the Ni(3)−O chains are further interconnected via Ni(1)−O(4)−Ni(3) and Ni(2)−O(9)−Ni(3) bridges into a 3D network framework with large 12-MR tunnels along the *a*-axis. The Ni···Ni separations between edge-sharing NiO_6 octahedra are in the range of 3.037(1)−3.064(1) Å whereas those between two corner-sharing NiO_x (x = 5, 6) are in the range of 3.170(1)−3.592(1) Å (Table 2). The MoO_4 and TeO_3 polyhedra are capped on the walls of the 12-MR tunnels (Figure 5).

Both TeO_3 groups are hexadentate and bridge with six nickel(II) ions, each oxygen atom is bidentate. Each MoO_4 tetrahedron connects with five nickel(II) ions by using three of its four oxygens, two of them are bidendate whereas the third one is unidentate, the fourth oxygen is orientated toward the center of the 12-MR tunnel.

It is interesting to compare the structures of $Ni_3(MoO_4)(TeO_3)_2$ and $Ni_3(Mo_2O_8)(XO_3)$ (X = Se, Te) reported previously by our group.[15a] The Ni−O architectures in three compounds are different: $[Ni_6O_{22}]^{32-}$ hexanulear clusters in $Ni_3(Mo_2O_8)(SeO_3)$, 1D nickel oxide chains in $Ni_3(Mo_2O_8)(TeO_3)$ and 3D network in $Ni_3(MoO_4)(TeO_3)_2$. Furthermore, the $[Mo_4O_{16}]^{8-}$ clusters were observed in $Ni_3(Mo_2O_8)(XO_3)$ (X = Se, Te) whereas the MoO_4 tetrahedra in $Ni_3(MoO_4)(TeO_3)_2$ remain “isolated”.

Optical Properties. The infrared spectra of $Mn(MoO_3)(SeO_3)(H_2O)$, $Co(MoO_3)(SeO_3)(H_2O)$, $Fe_2(Mo_2O_7)(SeO_3)_2(H_2O)$, $Cu_2(MoO_4)(SeO_3)$, and $Ni_3(MoO_4)(TeO_3)_2$ display similar features (see Supporting Information). They revealed the Se−O, Te−O and Mo−O vibrations between 400 and 1000 cm^{-1}. The bands between 800 and

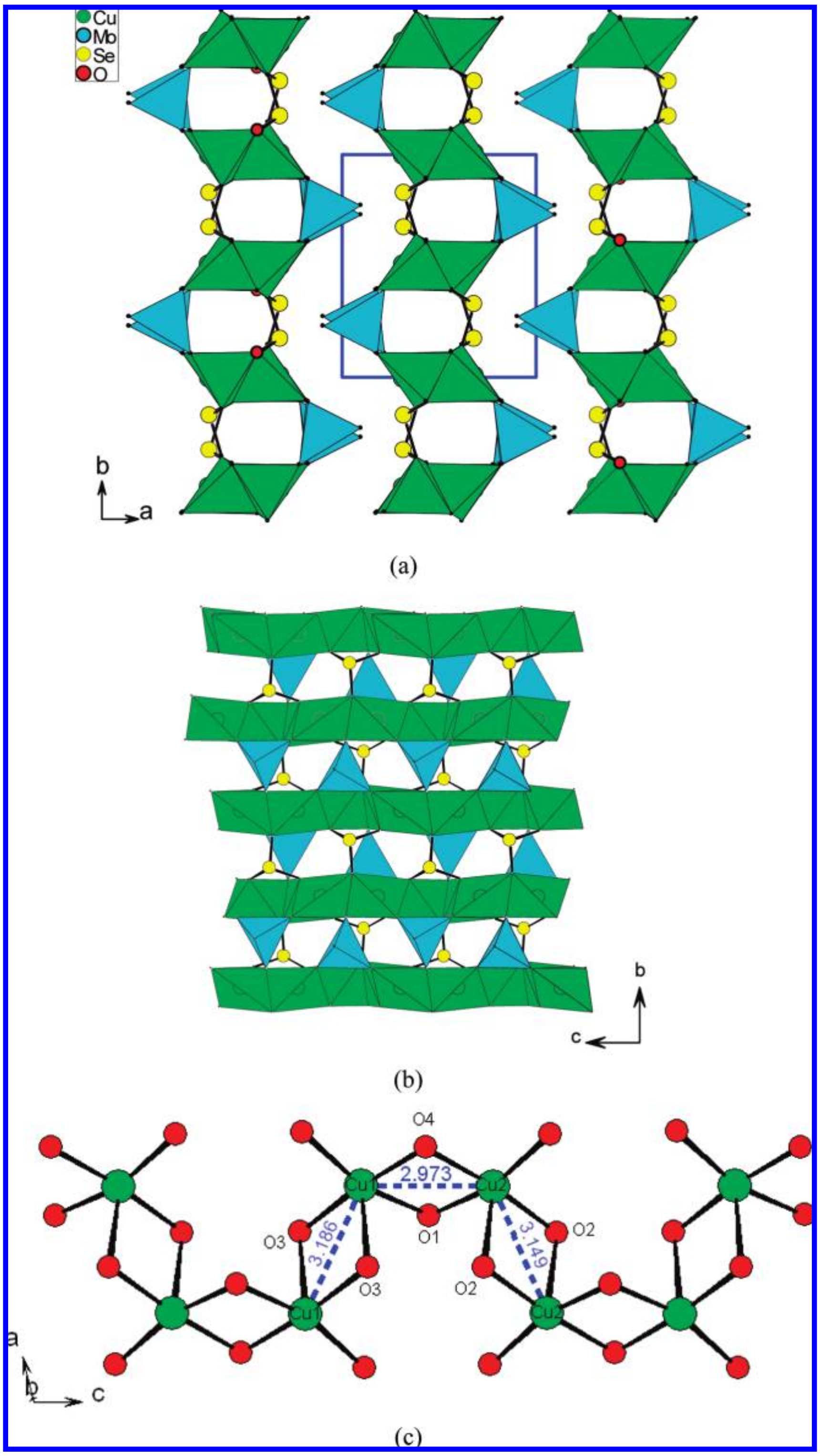

(a)

(b)

(c)

Figure 4. View of the structure of $Cu_2(MoO_4)(SeO_3)$ down the *c*-axis (a), a 2D $Cu_2(MoO_4)(SeO_3)$ layer perpendicular to the *a*-axis (b), and a 1D copper oxide chain composed of edge-sharing CuO_5 square pyramids along the *c*-axis (c).

940 cm^{-1} and those between 550 and 600 cm^{-1} can be assigned to *v*(Mo−O) vibrations, whereas the bands between 600 and 800 cm^{-1} are originated from *v*(Te−O) or *v*(Se−O) vibrations. The bands from 400 to 550 cm^{-1} may be assigned to *v*(Te−O−Te) or *v*(Se−O−Se). For $Mn(MoO_3)(SeO_3)(H_2O)$, $Co(MoO_3)(SeO_3)(H_2O)$, and $Fe_2(Mo_2O_7)(SeO_3)_2(H_2O)$, the bands in the range of 3000−3500 cm^{-1} can be assigned to *v*(H−O−H) whereas the bands in the range 1400−1650 cm^{-1} are characteristic of *v*(O−H). All of the assignments are consistent with those previously reported.[26]

UV absorption spectra revealed several absorption peaks in the range of 190−2500 nm for $Co(MoO_3)(SeO_3)(H_2O)$, $Fe_2(Mo_2O_7)(SeO_3)_2(H_2O)$, $Cu_2(MoO_4)(SeO_3)$,

---

[26] (a) Ok, K. M.; Halasyamani, P. S. *Chem. Mater.* **2006**, *18*, 3176. (b) Harrison, W. T. A.; Dussack, L. L.; Jacobson, A. J. *Inorg. Chem.* **1994**, *33*, 6043.

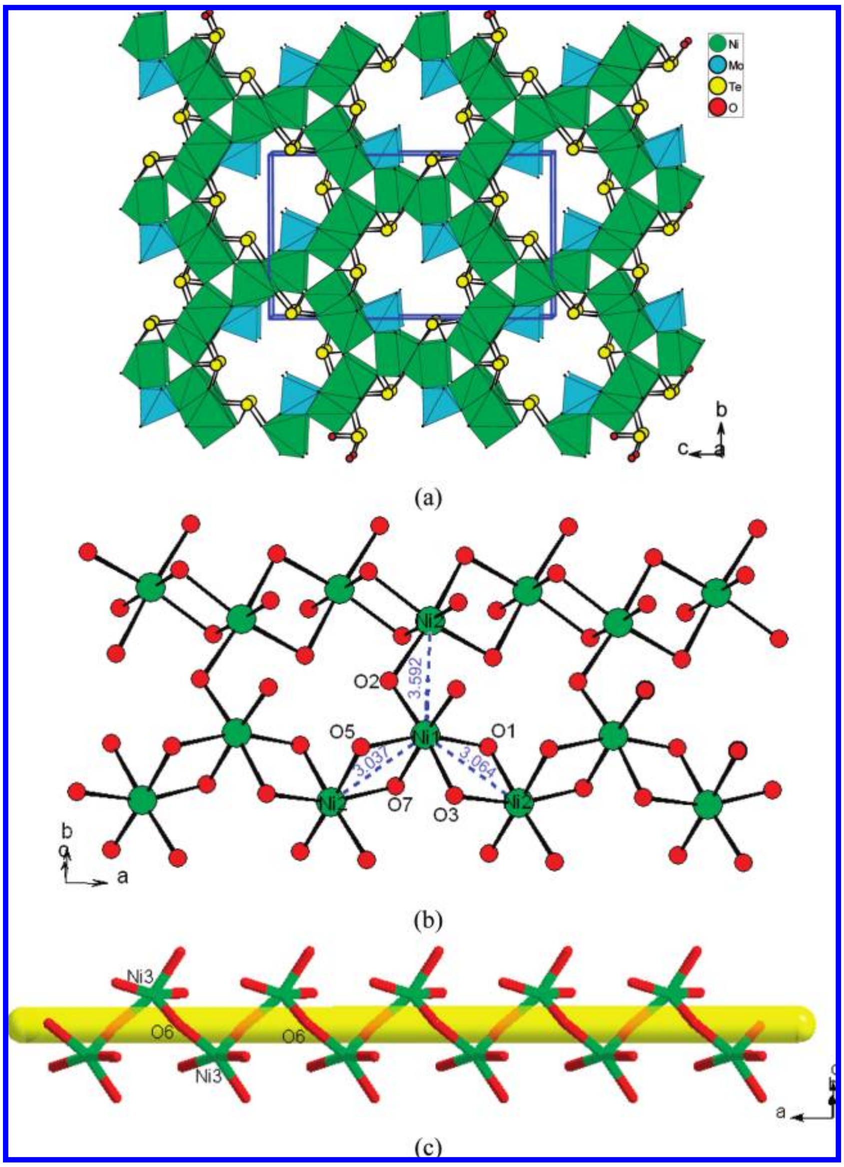

Figure 5. View of the structure of $Ni_3(MoO_4)(TeO_3)_2$ down the *a*-axis (a); the nickel oxide layer parallel to the *ab* plane composed of $Ni(1)O_6$ and the $Ni(2)O_6$ octahedra connected via corner- and edge- sharing (b), the right-hand helical nickel oxide chain composed of corner-sharing $Ni(3)O_5$ polyhedra along the *a*-axis (c).

and $Ni_3(MoO_4)(TeO_3)_2$ whereas $Mn(MoO_3)(SeO_3)(H_2O)$ shows little absorption in the range of 600−2500 nm. Optical diffuse reflectance spectra indicate that all five compounds are semiconductors, and revealed a band gap of 2.10, 2.32, 2.25, 2.55, and 2.25 eV, respectively (see Supporting Information).

Thermogravimetric Analysis (TGA). TGA under a nitrogen atmosphere indicates that $Mn(MoO_3)(SeO_3)(H_2O)$, $Co(MoO_3)(SeO_3)(H_2O)$, $Fe_2(Mo_2O_7)(SeO_3)_2(H_2O)$, $Cu_2(MoO_4)(SeO_3)$, and $Ni_3(MoO_4)(TeO_3)_2$ are stable up to 300, 375, 375, 475, and 750 °C, respectively (Figure 6).

$Mn(MoO_3)(SeO_3)(H_2O)$ and $Co(MoO_3)(SeO_3)(H_2O)$ exhibit one main step of weight loss. The weight loss in 320−640 °C corresponds to the release of one mol of SeO_2 and one mol of H_2O molecules per formula unit. The observed weight loss of 39.6% for $Mn(MoO_3)(SeO_3)(H_2O)$ is slightly larger than the calculated one (37.5%) whereas the observed weight loss of 36.0% for $Co(MoO_3)(SeO_3)(H_2O)$ is slightly lower than the calculated one (37.1%).

$Fe_2(Mo_2O_7)(SeO_3)_2(H_2O)$ and $Cu_2(MoO_4)(SeO_3)$ exhibit two main steps of weight loss. For $Fe_2(Mo_2O_7)(SeO_3)_2(H_2O)$, the first step in the temperature range of 375−560 °C corresponds to the release of 2 mol of SeO_2 and 1 mol of H_2O per formula unit. The observed weight loss of 35.7% is close to the calculated one (34.9%). Above 560 °C, $Fe_2(Mo_2O_7)(SeO_3)_2(H_2O)$ is further decomposed. The total weight loss at 1000 °C is 39.8%, and the final residuals were not characterized because of their melting under such high temperature with the TGA bucket made of Al_2O_3. For $Cu_2(MoO_4)(SeO_3)$, the first step of weight loss in the temperature ranges of 560−600 °C corresponds to the release of 1 mol of SeO_2 per formula unit. The second step of weight loss in the temperature ranges of 760−870 °C corresponds to the further decomposition of the compound. The observed total weight loss at 1000 °C is 29.4%, and the final

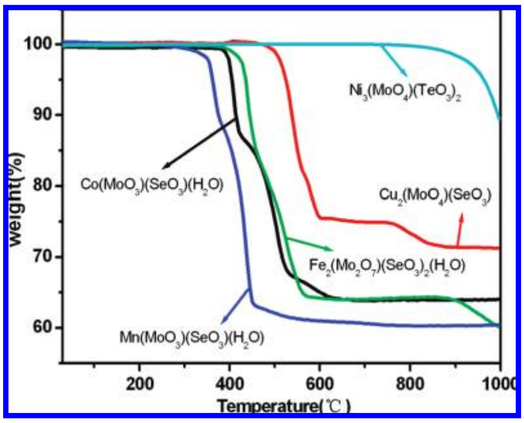

Figure 6. TGA curves of $Mn(MoO_3)(SeO_3)(H_2O)$(blue), $Co(MoO_3)(SeO_3)(H_2O)$(black), $Fe_2(Mo_2O_7)(SeO_3)_2(H_2O)$(green), $Cu_2(MoO_4)(SeO_3)$ (red), and $Ni_3(MoO_4)(TeO_3)_2$ (cyan).

residuals were not characterized because of the same reason we mentioned earlier.

$Ni_3(MoO_4)(TeO_3)_2$ exhibits one main step of weight loss, which can be attributed to the release of TeO_2 molecules. The total weight loss at 1000 °C is about 10.5%. From the slopes of the curve, it is clear that the decomposition has not ended at 1000 °C. The final residuals were not characterized because of their melting under such high temperature with the TGA bucket made of Al_2O_3.

Magnetic Properties. The temperature-dependent magnetic susceptibilities of $Mn(MoO_3)(SeO_3)(H_2O)$, $Co(MoO_3)(SeO_3)(H_2O)$, $Fe_2(Mo_2O_7)(SeO_3)_2(H_2O)$, $Cu_2(MoO_4)(SeO_3)$, and $Ni_3(MoO_4)(TeO_3)_2$ were measured at 1000 or 5000 Oe in the temperature range 2−300 K.

$Mn(MoO_3)(SeO_3)(H_2O)$ obeys the Curie−Weiss law in the temperature range of 2−300 K (Figure 7a). At 300 K, the $\chi_M T$ value of 4.33 emu·mol^{-1}·K corresponds to an effective magnetic moment (μ_{eff}) of 5.886 μ_B for one isolated Mn^{2+} (S = 5/2, g = 1.99) ions.[27] The $\chi_M T$ value decreases continuously upon cooling and reaches a value of 0.38 emu·mol^{-1}·K at 2.0 K. Linear fit of the magnetic data according to the Curie−Weiss law in the range of 2−300 K gave a Weiss constant (θ) of −12.8(5) K, indicating antiferromagnetic interactions between Mn(II) centers. It is expected that the magnetic interaction occurred mainly between magnetic centers within the 1D manganese(II) selenite chains discussed in the previous section.

$Co(MoO_3)(SeO_3)(H_2O)$ obeys the Curie−Weiss law in the temperature range of 2−300K (Figure 7b). At 300 K, the $\chi_M T$ value of 2.78 emu·mol^{-1}·K corresponds to an effective magnetic moment (μ_{eff}) of 4.715 μ_B for an isolated Co^{2+} (S = 3/2, g = 2.435) ion per formular unit.[28] The $\chi_M T$ value decreases continuously upon cooling and reaches a value of 0.17 emu·mol^{-1}·K at 2.0 K. A linear fit of the magnetic data in the range of 50−300 K gave a Weiss constant (θ) of −2.43(3) K, indicating very weak antiferromagnetic interactions between magnetic centers. It is expected that the magnetic interaction occurred mainly between magnetic centers bridged by a pair of selenite anions within the 1D cobalt(II) selenite chain.

$Fe_2(Mo_2O_7)(SeO_3)_2(H_2O)$ obeys the Curie−Weiss law in the temperature range of 50−300 K; below 50 K a slight deviation was observed (Figure 7c). At 300 K, the $\chi_M T$ value is 3.95 emu·mol^{-1}·K, which corresponds to an effective magnetic moment (μ_{eff}) of 5.650 μ_B for one isolated Fe^{3+} (S = 5/2, g = 1.91) ions.[29] The $\chi_M T$ value decreases continuously upon cooling and reaches a value of 0.075 emu·mol^{-1}·K at 2.0 K. A linear fit of the magnetic data according to the Curie−Weiss law in the range of 50−300 K gave a Weiss constant (θ) of −119.9(8) K, indicating very strong antiferromagnetic interactions between Fe(III) centers. The magnetic interactions are mainly within the Fe_2O_{10} dimeric unit as well as intracluster magnetic interaction within the iron(III) selenite layer (Figure 3b). The intracluster Fe···Fe separation is 3.142(1) Å, and the shortest intercluster Fe···Fe separation is 4.715(1) Å.

$Cu_2(MoO_4)(SeO_3)$ obeys the Curie−Weiss law in the temperature range of 100−300 K, below 100 K; a slight deviation was observed (Figure 7d). At 300 K, the $\chi_M T$ value is 0.815 emu·mol^{-1}·K, which corresponds to an effective magnetic moment (μ_{eff}) of 1.80 μ_B for two isolated Cu^{2+} (S = 1/2, g = 2.08) ions.[30] The $\chi_M T$ value decreases continuously upon cooling and reaches a value of 0.019 emu·mol^{-1}·K at 2.0 K. A linear fit of the magnetic data in the range of 100−300 K gave a Weiss constant (θ) of −71.2(7) K, indicating significant antiferromagnetic interactions between magnetic centers. The magnetic interactions should be dominated by the magnetic exchange interactions between edge-sharing CuO_5 square pyramids within the 1D copper(II) oxide chain (Figure 4c).

$Ni_3(MoO_4)(TeO_3)_2$ obeys the Curie−Weiss law in the temperature range of 50−300 K; below 50 K a slight deviation is observed (Figure 7e). At 300 K, the $\chi_M T$ value of 3.74 emu·mol^{-1}·K corresponds to an effective magnetic moment (μ_{eff}) of 5.47 μ_B for three isolated Ni^{2+} (S = 1, g = 2.327) ions per formular unit.[31] The $\chi_M T$ value decreases continuously upon cooling, and a value of 0.15 emu·mol^{-1}·K is reached at 2.0 K. A linear fit of the magnetic data in the range of 50−300 K gave a Weiss constant (θ) of −24.9(3) K, indicating significant antiferromagnetic interactions between magnetic centers. It is expected that the magnetic interactions are mainly between two Ni(II) ions interconnected via corner- or edge-sharing within the 3D nickel(II) oxide network (Figure 5a).

SHG Measurements. $Mn(MoO_3)(SeO_3)(H_2O)$ and $Ni_3(MoO_4)(TeO_3)_2$ crystallize in NCS space groups ($Pmc2_1$ and $P2_12_12_1$). Hence, their second-order NLO properties are worth studying. SHG measurements on a Q-switched Nd:YAG laser on the sieved-powder sample (80−100 mesh) indicate that $Mn(MoO_3)(SeO_3)(H_2O)$ displays a moderately strong SHG signal about 3 times that of

---

(27) Larrañaga, A.; Mesa, J. L.; Pizarro, J. L.; Lezama, L.; Chapman, J. P.; Arriortua, M. I.; Rojo, T. *Dalton Trans* . **2005**, 1727.

(28) Becker, R.; Berger, H.; Johnsson, M.; Prester, M.; Marohnic, Z.; Miljak, M.; Herak, M. *J. Solid State Chem.* **2006**, *179*, 836.

(29) Becker, R.; Johnsson, M.; Kremer, R. K.; Klauss, H. H.; Lemmens, P. *J. Am. Chem. Soc.* **2006**, *128*, 15469.

(30) Johnsson, M.; Törnroos, K. W.; Mila, F.; Millet, P. *Chem. Mater.* **2000**, *12*, 2853.

(31) Johnsson, M.; Törnroos, K. W.; Lemmens, P.; Millet, P. *Chem. Mater.* **2003**, *15*, 68.

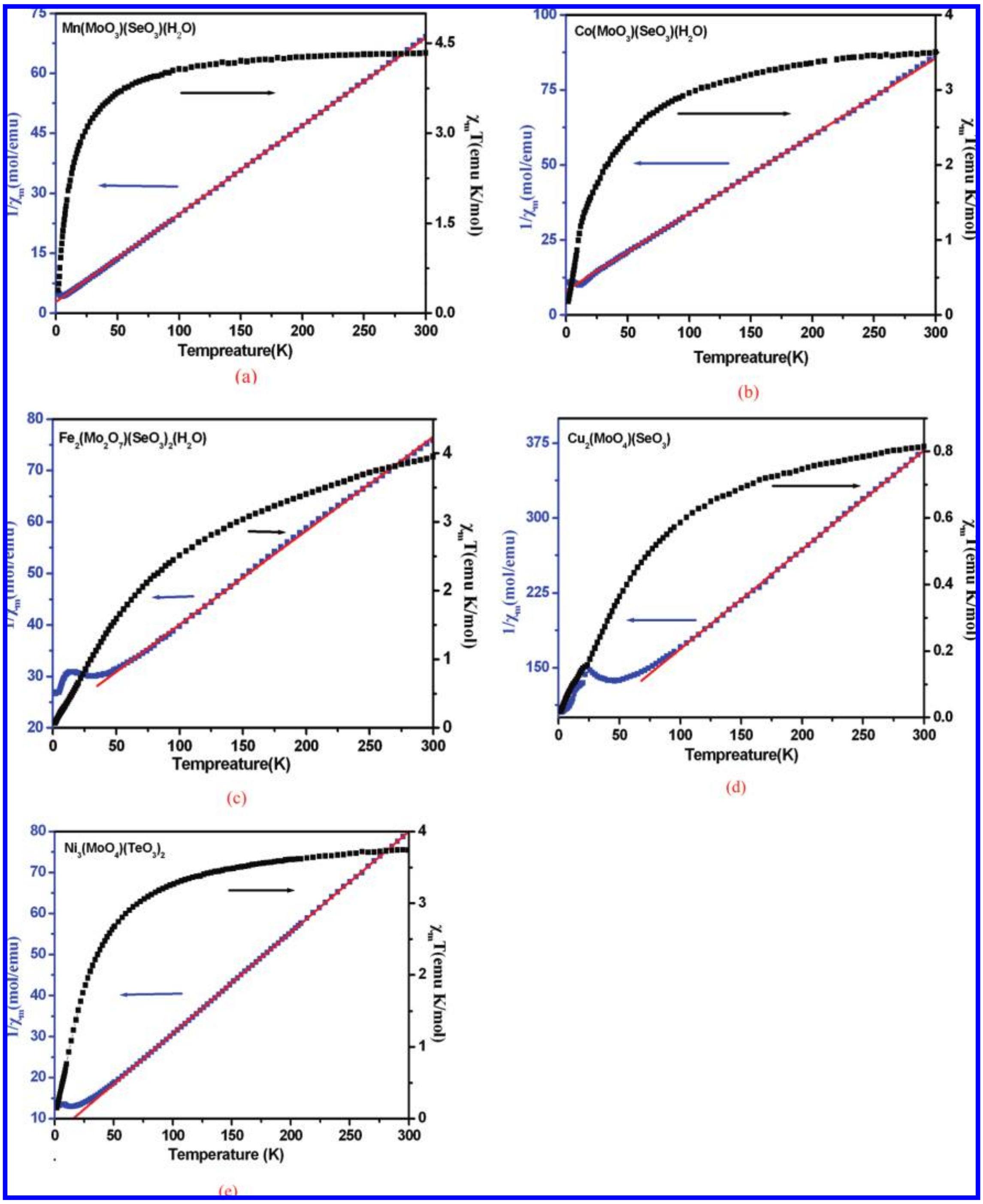

Figure 7. 1/χ versus T and χT versus T plots for Mn(MoO$_3$)(SeO$_3$)(H$_2$O) (a), Co(MoO$_3$)(SeO$_3$)(H$_2$O) (b), Fe$_2$(Mo$_2$O$_7$)(SeO$_3$)$_2$(H$_2$O) (c), Cu$_2$(MoO$_4$)(SeO$_3$) (d), and Ni$_3$(MoO$_4$)(TeO$_3$)$_2$ (e). The red lines represent the linear fits of data according to the Curie−Weiss law.

KDP whereas the SHG signal of Ni$_3$(MoO$_4$)(TeO$_3$)$_2$ is much weaker than that of KDP.

To understand the origin of the SHG response, the distortion and polarization of both Mo−O and Se(Te)−O bonds in both compounds were analyzed. In Mn(MoO$_3$)(SeO$_3$)(H$_2$O), both Mo^{6+} and Se^{4+} are in asymmetric coordination environments owing to second-order Jahn−Teller distortions (see Supporting Information). The "net" direction of both types of distortion is along the (0 1 −1) direction; hence, a moderate SHG response resulted. For Ni$_3$(MoO$_4$)(TeO$_3$)$_2$, the Mo^{6+} with a tetrahedral geometry has little contribution to the SHG effect. The polarizations of the tellurite groups also almost canceled each other (Figure 5a). Hence, Ni$_3$(MoO$_4$)(TeO$_3$)$_2$ gave a much weaker SHG response than that of Mn(MoO$_3$)(SeO$_3$)(H$_2$O).

Conclusions

In summary, five new transition metal molybdenum(VI) selenites or tellurites, namely, TM(MoO$_3$)(SeO$_3$)(H$_2$O) (TM = Mn, Co), Fe$_2$(Mo$_2$O$_7$)(SeO$_3$)$_2$(H$_2$O), Cu$_2$(MoO$_4$)(SeO$_3$), and Ni$_3$(MoO$_4$)(TeO$_3$)$_2$ have been prepared and structurally characterized. They display five different types of 3D networks and a 2D layered architecture. The selenite or tellurite anions are able to adopt many types of coordination modes. In TM(MoO_3)(SeO_3)(H_2O) (TM = Mn, Co) and Fe_2(Mo_2O_7)(SeO_3)$_2$(H_2O), the selenite anions are bonded to both transition metal ions and Mo^{6+} cations, whereas selenite anions in Cu_2(MoO_4)(SeO_3) and tellurite anions in Ni_3(MoO_4)(TeO_3)$_2$ are only involved in coordination with Cu(II) or Ni(II) ions. The MoO_6 octahedra in the first three compounds are distorted toward an edge or a face, furthermore they are able to form 1D chains via corner- or edge-sharing. In Ni_3(MoO_4)(TeO_3)$_2$ and Cu_2(MoO_4)(SeO_3), the Mo^{6+} cations are tetrahedrally coordinated, and those MoO_4 tetrahedra are capped on the transition metal selenite or tellurite frameworks. Mn(MoO_3)(SeO_3)(H_2O) displays a SHG signal about 3 times that of KDP, whereas the SHG signal of Ni_3(MoO_4)(TeO_3)$_2$ is much weaker than that of KDP. Our future research efforts will be devoted to further explorations of new SHG materials in other transition metal compounds with two types of second-order Jahn−Teller distortions.

Acknowledgment. This work was supported by National Natural Science Foundation of China (Nos. 20731006, 20825104, and 20821061) and the Knowledge Innovation Program of the Chinese Academy of Sciences.

Supporting Information Available: X-ray crystallographic files in CIF format, simulated and experimental XRD powder patterns, IR spectra, and optical diffuse reflectance spectra for Mn(MoO_3)(SeO_3)(H_2O), Co(MoO_3)(SeO_3)(H_2O), Fe_2(Mo_2O_7)(SeO_3)$_2$(H_2O), Cu_2(MoO_4)(SeO_3), and Ni_3(MoO_4)(TeO_3)$_2$. This material is available free of charge via the Internet at http://pubs.acs.org.